



Evaluation of the Stability of Argan Oil Nanoemulsions Formulated and Optimized through Experimental Design for Dermatological Applications

Yousra Mdarhri^{1*}, Ikram Bouziane¹, Narjisse Mokhtari¹, Lama Rissouli¹, Ahmed Touhami², Fakhita Touhami³, Mohamed Chabbi¹

¹Department of Chemistry, Faculty of Science and Technology of Tangier, Abdelmalek Essaâdi University, Tetouan 93000, Morocco

²Department of Physics & Astronomy, College of Sciences, University of Texas Rio Grande Valley, Edinburg, TX 78539, USA

³Information and Communication Systems Department, National School of Applied Sciences, Abdelmalek Essaâdi University, Tetouan 93000, Morocco

ARTICLE INFO

Article history:

Received 10 November 2024

Received 18 November 2024

Accepted 27 November 2024

Published online 01 January 2025

ABSTRACT

Argan oil is a highly sought-after natural product renowned for its therapeutic and rejuvenating properties. This study focused on harnessing its dermatological bioactivity by developing stable nanoemulsions through a simple low-energy method using a single non-ionic surfactant. The composition and properties of Argan oil were analyzed using High-Performance Liquid Chromatography (HPLC), Gas Chromatography (GC), and quality indexes, adhering to international standards. The effect of system composition on stability was evaluated using a pseudo-ternary phase diagram and Phase Inversion Composition (PIC) emulsification technique. Optimal process parameters for producing stable nanoemulsion were determined through Response Surface Methodology (RSM) analysis. The resulting nanoemulsions were characterized for storage stability, average droplet size, and Polydispersity Index (PDI) using Dynamic Light Scattering (DLS). The physicochemical properties and bioactive compounds of Argan oil were identified, including a total tocopherol content of 841 ± 35 mg/kg and a total phenolic content of 83.81 ± 0.71 mg Gallic Acid Equivalent (GAE) per kg of oil, highlighting its dermatological potential. The ideal composition was established, and phase behavior was monitored alongside process parameters to ensure the formation of stable nanoemulsion. Stability analysis confirmed the physical stability of the nanoemulsion over time under various storage conditions. Size analysis revealed a small average droplet size (130.154 ± 0.115 nm) and a narrow droplet size distribution (0.019 ± 0.003 nm). The low-energy PIC emulsification method successfully produced stable Argan oil nanoemulsions using low-speed stirring and a single non-ionic surfactant, requiring no additional compounds.

Keywords: Nanoemulsions, Argan oil, Low-energy emulsification, Response surface methodology, Box-Behnken.

Copyright: © 2024 Mdarhri *et al.* This is an open-access article distributed under the terms of the [Creative Commons Attribution License](https://creativecommons.org/licenses/by/4.0/), which permits unrestricted use, distribution, and reproduction in any medium, provided the original author and source are credited.

Introduction

The Argan tree (*Argania Spinosa* L. Skeels) is a remarkable species native to Morocco, where it holds great importance for both the local ecosystem and communities. This tree holds immense ecological value also playing a vital role socially and economically, largely due to its oil. Argan oil, a premium vegetable oil, is extracted from the kernels of the Argan tree through traditional methods that avoid the use of solvents or heat, ensuring the preservation of its natural properties. Renowned for its numerous benefits, Argan oil is widely used in cosmetic and pharmaceutical products.¹ Argan oil is rich in a diverse range of beneficial compounds, including unsaturated and saturated fatty acids, polyphenols, tocopherols, chlorophylls, carotenoids, phytosterols, squalene, and coenzyme Q10.¹⁻³ These components work together to deliver a variety of bioactive effects.

Renowned for its hydrating properties, Argan oil enhances skin elasticity, offers anti-aging benefits, and aids in healing burn wounds while reducing inflammation. Additionally, Argan oil serves as a treatment for various dermatological conditions, including acne, psoriasis, eczema, and blisters.^{1,4-6} To maximize its benefits and preserve its integrity, Argan oil can be effectively encapsulated in dermatological emulsion formulations. This approach not only helps to preserve its quality but also improves its efficacy, by enabling a targeted and sustained release of its bioactive compounds when applied to the skin. As a natural powerhouse, Argan oil offers numerous advantages for skin health and overall wellness. Nanoemulsions show a great potential for targeted applications in industries such as pharmaceuticals, cosmetics, and food. Nanoemulsions containing vegetable oils, such as Argan oil, olive oil, and palm oil, have been the subject of various studies.⁷⁻⁹ Particularly, nanoemulsions are used as drug delivery systems due to their advantages over other methods, including their ultrafine dispersions and differential drug-loading properties. Nanoemulsions have been applied as drug delivery vehicles for several systemic routes, including ocular, nasal, oral, topical, transdermal, transmucosal, and parenteral routes.¹ For instance, the main benefit for employing nanoemulsions in dermal applications is their ability to enhance skin penetration and permeation through both the skin and the pilosebaceous unit without the need for penetration enhancer.^{10,11} In these applications, evaluating nanoemulsion stability is crucial. Stability testing involves assessing the system's ability to maintain its desired state over time using various methods like, visual inspection, centrifugation, accelerated stability tests, storage stability analysis, creaming rate determination, and particle size analysis. Instability issues can significantly affect nanoemulsion performance.¹² These

*Corresponding author. E mail: yousra.mdarhri@gmail.com
Tel: +212649967627

Citation: Mdarhri Y, Bouziane I, Mokhtari N, Rissouli L, Touhami A, Touhami F, Chabbi M. Evaluation of the Stability of Argan Oil Nanoemulsions Formulated and Optimized through Experimental Design for Dermatological Applications. Trop J Nat Prod Res. 2024; 8(12): 9414 – 9421 <https://doi.org/10.26538/tjnpr/v8i12.9>

Official Journal of Natural Product Research Group, Faculty of Pharmacy, University of Benin, Benin City, Nigeria

changes may be influenced by the components, their proportions, formulation techniques, and environmental conditions.

The emulsification process by Phase Inversion Composition (PIC) is a low-energy preparation method that involves gradually adding one phase to another while stirring continuously at constant temperature. This technique relies on the critical balance of components that causes the inversion of the continuous and dispersed phases enabling emulsification without the need for high shear mixing. Emulsifying agents stabilize the system by forming an interface at the surface of the droplets.¹³

The nanoemulsion formulation process can be strategically planned using the Design of Experiments (DOE) method, also known as experimental design. This method involves studying how different process variables affect the characteristics of the nanoemulsion system. Additionally, the pseudo-ternary phase diagram is a valuable tool that provides insights into how different components and their proportions influence the phase behavior and properties of the prepared systems. This approach aids in selecting optimal mixtures and designing formulations with desired characteristics. Response Surface Methodology (RSM), statistical and mathematical approach, is applied to develop, improve, and optimize multivariate processes by analyzing how input variables might influence the process and identifying those that significantly impact system's output. Several studies have used RSM to stabilize and optimize nanoemulsion formulation.^{14,17,18}

This study represents a novel contribution aimed at enhancing the value of Argan oil through the synthesis and characterization of Argan oil-based nanoemulsions. The formulation uses a non-ionic surfactant and a simple low-energy method. This was achieved through a screening approach that examined the composition of oil and surfactant, as indicated by the pseudo-ternary phase diagram. The production conditions of these Argan oil nanoemulsions were further optimized by adjusting process parameters, using Response Surface Methodology. Further research is recommended to explore the bioactive properties of these nanoemulsions and their potential pharmaceutical applications.

Materials and Methods

Materials

Unroasted Argan kernels were acquired from the Arganeraie Biosphere Reserve (RBA) in Morocco. The following reagents were used in the study: Tween 20 (Loba Chemie); diethyl ether, potassium iodide, cyclohexane, iodine monochloride, hydrochloric acid, acetone, isooctane, and sodium carbonate (Honeywell); sodium thiosulfate (Labkem); acetonitrile (Fisher Scientific); and ethanol, potassium hydroxide, phenolphthalein, chloroform, acetic acid, starch, methanol, hexane, folin-ciocalteu reagent, p-anisidine, gallic acid, fatty acid methyl esters, and tocopherols (Sigma-Aldrich). All reagents were of extra-pure, analytical, or HPLC grade.

Oil Characterization

Argan oil (*Argania Spinosa* L. Skeels) was extracted through mechanical cold pressing of unroasted Moroccan Argan kernels. The oil yield was calculated based on the weight of kernels and the amount of oil produced. Its physicochemical properties were analyzed in accordance with international standards, including: acid value and free fatty acid content (ISO 660),¹⁹ peroxide value (International Olive Council Standard),²⁰ specific ultraviolet extinction (ISO 3656),²¹ iodine value (ISO 3961),²² saponification value (ISO 3657),²³ unsaponifiable matter (ISO 3596),²⁴ relative density at 20°C (ISO 6883),²⁵ refraction index (ISO 6320),²⁶ moisture and volatile matter (ISO 662),²⁷ insoluble impurities (ISO 663),²⁸ anisidine value, and total oxidation value (ISO 6885).²⁹

The fatty acid composition of the oil was determined using Gas Chromatography (GC) (Ultra GC Trace Thermo-Fischer, France) with a CP-SIL 5CB capillary column (0.32 mm x 50 m x 1.20 µm) following the International Olive Council Standard Method.³⁰ Tocopherol content was determined using High-Performance Liquid Chromatography (HPLC) (HPLC-DAD Shimadzu, Japan) with Wakosil C18HG column (5 µm, 4.6 x 150 mm) in accordance with ISO 9936.³¹ Total phenolic content was measured a modified Folin-Ciocalteu procedure using Gallic acid as the standard.³² Pigment content was measured

spectrophotometrically using a UV-2005 Spectrophotometer (J.P. Selecta, Spain).³³

Construction of Pseudo-Ternary Phase Diagram

A pseudo-ternary phase diagram was constructed by mixing Argan oil, Tween 20, and water using the aqueous titration method.³⁴ Initially, nine oil-to-surfactant ratios (ranging from 1:9 to 9:1 w/w) were prepared. Bi-distilled water was gradually added dropwise to each mixture at room temperature adjusting the water concentration from 9% to 95% of the total weight in intervals of 3-7%. Each sample was stirred for 40 minutes at 1500 rpm using a magnetic stirrer and then allowed to equilibrate at room temperature for 24 hours. The physical state of each sample was visually inspected, and combinations without phase separation were identified and plotted on the pseudo-ternary phase diagram.

Evaluation of Formulations

Thermodynamic Stability, Storage Stability, and Creaming Index

Thermodynamic stability was evaluated using several stress tests: centrifugation at 3000 rpm for 30 minutes, freeze-thaw cycles (-20°C / +25°C), and heating-cooling cycles (4°C / 40°C). The formulations were stored for four months under different conditions—refrigeration (4 ± 1°C), room temperature (25°C ± 1°C), and in a hot air oven (40 ± 1°C)—to monitor storage stability until phase separation occurred, forming a top opaque layer and a transparent lower layer. Destabilization at 40°C was quantified using the creaming index calculated as the percentage of the lower layer height relative to the total formulation height.³⁵

pH, Droplet Size, and Polydispersity Index

The apparent pH was measured immediately after homogenization, while particle size analysis was performed using light scattering (Nano DS Cilas, France) 24 hours after preparation, at ambient temperature.

Response Surface Experimental Design

A Box-Behnken response surface experimental design was developed to investigate the effects of various operational parameters on the properties of nanoemulsions.³⁶ This design incorporated three factors at three levels, which is suitable for studying quadratic response surfaces and generating second-order polynomial models. The independent variables were mixing temperature (X_1), mixing time (X_2), and stirring velocity (X_3), while the dependent variable was the average droplet size of the nanoemulsion (Y). The variable levels—high (+1), medium (0), and low (-1)—are detailed in Table 1. The experimental design produced a second-degree polynomial equation for average droplet size, represented as Equation (1):

$$Y = a_0 + a_1X_1 + a_2X_2 + a_3X_3 + a_{11}X_1^2 + a_{22}X_2^2 + a_{33}X_3^2 + a_{12}X_1X_2 + a_{13}X_1X_3 + a_{23}X_2X_3 \quad (1)$$

Where Y is the dependent variable (average droplet size); X_1 , X_2 , and X_3 are the independent variables: mixing temperature, mixing time, and stirring velocity, respectively. The coefficients (a_0 , a_1 , a_2 , and a_3) represent the model constant and the linear effects of the independent variables; Quadratic effects are denoted by a_{11} , a_{22} , and a_{33} , while a_{12} , a_{13} , and a_{23} represent the interaction effects between the variables.

Statistical Analysis

Data were collected from duplicate or triplicate experiments using freshly prepared samples. Results are expressed as the mean ± standard deviation. Statistical analysis was conducted using analysis of variance (ANOVA) with Minitab®18 software. Means were compared using a T-test, with significance threshold set at a $p < 0.05$.

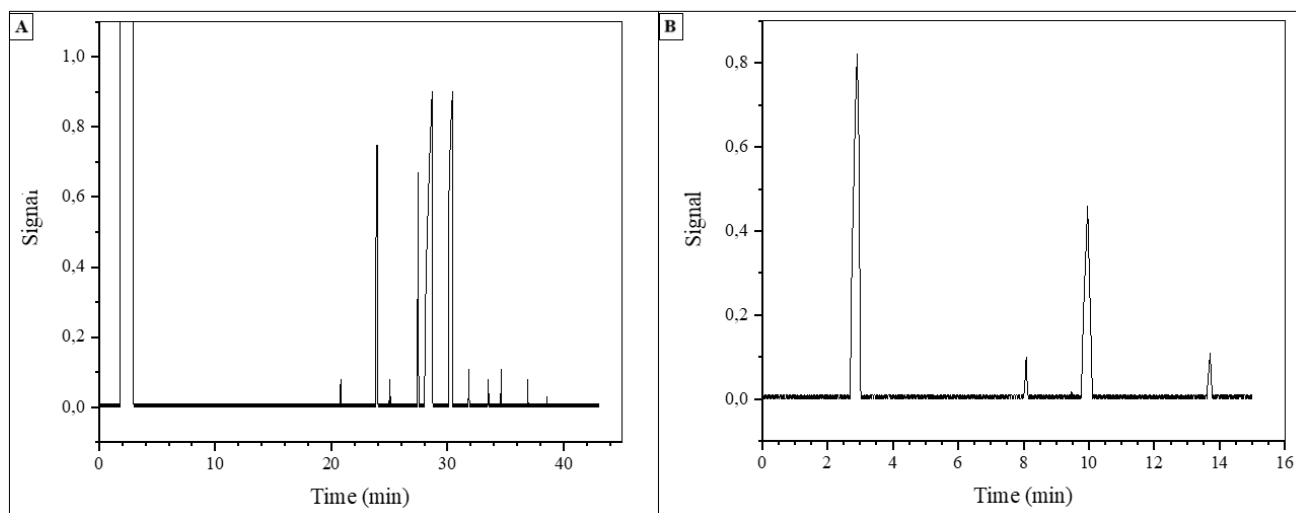
Results and Discussion

Oil Characterization

The fatty acid composition, tocopherol content, total phenolic content, and pigment content of Argan oil are summarized in Table 2, with the corresponding chromatograms of the fatty acid and tocopherol in Figure 1. Table 3 details the oil's extraction yield and physicochemical properties, including acid value, free fatty acid content, peroxide value,

Table 1: Design variables and their corresponding levels

Independent variables		Levels		
		(-1)	(0)	(+1)
X ₁	Mixing temperature (°C)	20	30	40
X ₂	Mixing time (min)	20	40	60
X ₃	Stirring velocity (rpm)	900	1250	1600
Dependent variables		Goals		
Y	Average droplet size (nm)	Minimize		

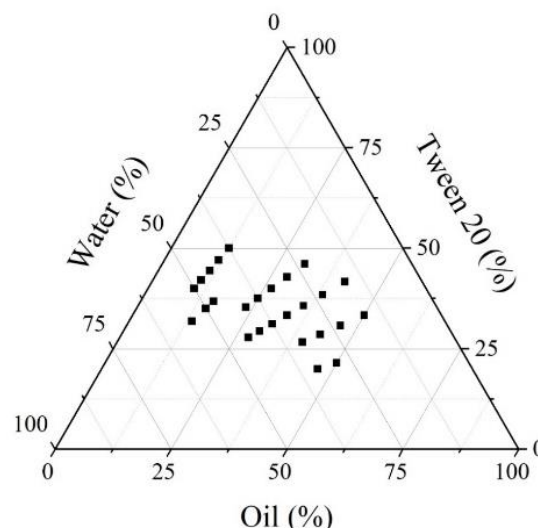
**Figure 1:** Oil composition chromatograms (A) fatty acid GC signal and (B) tocopherol HPLC signal

specific UV extinction, iodine value, saponification value, unsaponifiable matter, relative density (20°C), refraction index, moisture content, volatile matter, insoluble impurities, anisidine value, and total oxidation value. These characteristics were compared to the Moroccan specifications for Extra-Virgin Argan oil.³⁷

The results confirm that the bioactive composition (Table 2) and physicochemical properties (Table 3) meet the specifications for Extra Virgin Argan oil.³⁷ The fatty Acids, recognized for their anti-inflammatory properties, also enhance skin penetration, facilitating the delivery of both lipophilic and hydrophilic compounds.³⁸ The oil's pharmacological benefits stem from antioxidants, particularly polyphenols and tocopherols, which protect against oxidative stress from UV radiation and environmental pollutants.³⁹ Pigments further enhance oxidative stability under light-free conditions. These qualities make Argan oil a valuable component in skincare formulations. The high saponification value indicates the presence of shorter fatty acid chains, which are reactive and soluble, beneficial for cosmetic applications. Additionally, its refractive index exceeds that of the epidermis (1.44), suggesting suitability for protecting skin against solar damage.⁴⁰

Pseudo-Ternary Phase Diagram

The Pseudo-Ternary Phase diagram (Figure 2) revealed a central region of stable formulations after 24 hours, highlighting optimal stability conditions. Destabilization indicators such as creaming or phase separation, often assessed visually, arise from density differences or excessive droplet coalescence. Stable emulsions observed in this region underscore the efficacy of Tween 20 as a surfactant. It reduces interfacial tension and forms protective droplet barriers, maintaining emulsion homogeneity with minimal mechanical disruption. The non-ionic nature of Tween 20 enhances stratum corneum penetration and reduces skin irritation, making it suitable for dermatological applications.⁴¹

**Figure 2:** Pseudo-ternary phase diagram of one-phase formulations after 24h

Thermodynamic Stability, Storage Stability, and Creaming Index

Four formulations passed stability tests (Figure 3) and were monitored over four months (Table 4^{Error! Reference source not found.}). At 4°C, no phase separation or creaming occurred. At ambient temperature, destabilization began after several weeks, with sample 7D remaining stable for over two months. At 40°C,

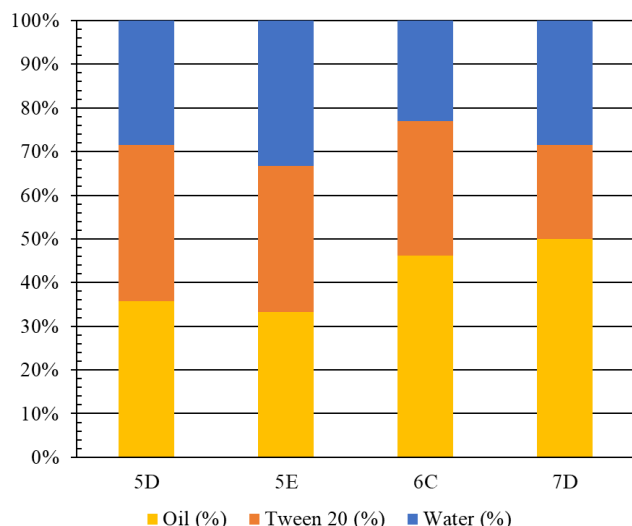


Figure 3: Oil, Tween 20, and water compositions of the selected formulations

destabilization occurred within days, with varying creaming indices. Stress testing identified meta-stable formulations and optimized stability conditions, indicating that low temperatures enhance stability by reducing droplet mobility. Sudden temperature changes can disturb the balance that keeps droplets stable, possibly impacting the performance and effectiveness of the surfactants. For long-term stability, formulations should preferably be stored at 4°C. Accelerated aging tests at 40°C simulated long-term storage, revealing that smaller droplets reduce gravitational separation and creaming.³⁵

pH, Average Droplet Size, and Polydispersity Index

The pH values recorded for all formulations were consistently within the acidic range, as detailed in Table 5. This observation is noteworthy, as the average droplet sizes recorded were within the nanometric scale, with the smallest droplets observed in formulation 7D. Additionally, these formulations exhibited low polydispersity indexes, indicating a high degree of uniformity in droplet size distribution. The pH values (Table 5) ranged from 4.0 to 5.5, aligning with the physiological range suitable for dermal applications. This range closely matches the natural pH of human skin, typically between 4.5 and 6.0.⁴² Such compatibility is vital for maintaining skin integrity, improving hydration, and reinforcing the skin's natural defense mechanisms against irritants and pathogens.

Table 2: Argan oil bioactive molecule composition in comparison with Moroccan regulations

Oil composition and physicochemical properties	Value	Extra Virgin Argan Oil
Fatty acids (g/100g)		
Myristic acid (C14:0)	0.1 ±0.0	<0.2
Palmitic acid (C16:0)	12.3 ±0.1	11.5 - 15.0
Margaric acid (C17:0)	0.0 ±0.0	Traces
Stearic acid (C18:0)	5.0 ±0.2	4.3 - 7.2
Arachidic acid (C20:0)	0.4 ±0.0	<0.5
Behenic acid (C22:0)	0.1 ±0.0	<0.2
Sum of Saturated Fatty Acids (FSA)	18.0 ±2.5	15.8 - 23.1
Palmitoleic acid (C16:1)	0.1 ±0.0	<0.2
Oleic acid (C18:1)	47.8 ±0.5	43.0 - 49.1
Gadoleic acid (C20:1)	0.4 ±0.0	<0.5
Sum of Monounsaturated Fatty Acids (MUFA)	48.3 ±7.4	43.0 - 49.8
Linoleic acid (C18:2)	33.5 ±0.4	29.3 - 36.0
Linolenic acid (C18:3)	0.1 ±0.0	<0.3
Sum of Polyunsaturated Fatty Acids (PUFA)	33.7 ±2.8	29.0 - 36.3
Tocopherols (mg/kg)		
α-tocopherol	57 ±6	18-75
β-tocopherol	2 ±0	1-5
γ-tocopherol	704 ±20	640 - 810
δ-tocopherol	78 ±9	54 - 110
Total Tocopherol content	841 ±35	600 - 900
Polyphenols (mg GAE/kg)		
Total phenolic content	83.81 ±0.71	-
Pigments (mg/kg)		
Carotenoids	0.39 ±0.00	-
Chlorophylls	0.44 ±0.01	-

Table 3: Argan oil physicochemical characterization in comparison with Moroccan regulations

Oil composition and physicochemical properties	Value	Extra Virgin Argan Oil
Extraction Yield (%)	51.42 ±0.03	-
Acid value (mg/g)	0.56 ±0.01	<1.6
Free fatty acid content (%)	0.28 ±0.01	<0.8
Peroxide value (mEqO ₂ / Kg)	2.9 ±0.1	<15.0
Specific ultraviolet extinction at 232 nm (K232)	1.33 ±0.04	<2.52
Specific ultraviolet extinction at 270 nm (K270)	0.24 ±0.02	<0.35
Specific ultraviolet extinction variation (ΔK)	0.00 ±0.00	<0.01
Iodine value (g/100g)	99.5 ±0.0	91.0 - 110.0
Saponification value (mg KOH/g)	194.9 ±0.1	189.0 - 199.1
Unsaponifiable matter (g/100 g)	0.87 ±0.01	<1.10
Relative density (20°C)	0.909 ±0.000	0.906 - 0.919
Refraction index (20°C)	1.4682 ±0.0004	1.463 - 1.472
Moisture and volatile compounds (%)	0.03 ±0.00	<0.10
Insoluble impurities content (%)	0.01 ±0.00	<0.30
Anisidine value	0.23 ±0.01	-
Total oxidation value	5.96 ±0.11	-

Table 4: Selected formulations: Oil-to-surfactant ratio, storage stability, and creaming index

Ref	Oil/Tween 20 ratio	Storage Stability (days)			Creaming Index (40°C) (%)
		4°C	25°C	40°C	
5D	1/1	>120	22	1	14.687 ±0.684
5E	1/1	>120	14	1	24.222 ±0.772
6C	3/2	>120	28	2	10.231 ±0.449
7D	7/3	>120	62	3	03.295 ±0.302

Table 5: Selected formulations: pH, droplet size, and polydispersity index

Ref	pH (25°C)	Average Droplet Size (nm)	PDI (nm)
5D	5.307 ±0.012	253.585 ±0.144	0.028 ±0.002
5E	5.047 ±0.015	323.060 ±0.212	0.041 ±0.003
6C	5.203 ±0.015	224.327 ±0.059	0.029 ±0.003
7D	4.830 ±0.017	130.154 ±0.115	0.019 ±0.003

The consistently small droplet sizes within the nanometer range contribute to the uniformity observed across all samples (see Table 5). Smaller droplets offer significant advantages, as they are less prone to coalescence and Ostwald ripening, both of which can undermine emulsion stability over time. This stability is supported by the positive correlation between droplet size and creaming index values; smaller droplets reduce gravitational separation, thereby lowering the creaming index and enhancing overall stability. Furthermore, the nanoemulsion droplets' small size facilitates better penetration into the skin, which is crucial for improved absorption and bioavailability of the active ingredients. This enhanced penetration not only boosts the efficacy of the formulations but also ensures the active components reach deeper skin layers, maximizing therapeutic benefits.⁴³

Response Surface Experimental Design

A Box-Behnken experimental design based on Response Surface Methodology (RSM) was employed to optimize formulation stability by evaluating the primary, interaction, and quadratic effects of operational variables on the average droplet size of a nanoemulsion.

The selected variables—mixing temperature, mixing time, and stirring velocity—were tested at three levels, resulting in 15 experiments: 12 at the edges of a multidimensional cubic design and three replicates at the center point. To minimize variability, the experiments were conducted in random order, and their conditions and responses are summarized in Table 6.

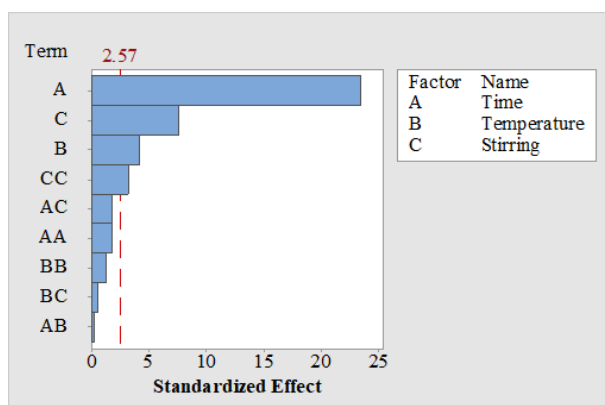
To assess the impact of the mixing temperature, mixing time, and stirring velocity on the average droplet size, a regression model was developed through analysis of variance (ANOVA). The resulting regression equation is presented in equation (2):

$$\text{Size (nm)} = 140.0 + 0.232 X_1 - 0.411 X_2 + 0.00218 X_3 - 0.00790 X_1^2 - 0.00256 X_2^2 - 0.000016 X_3^2 - 0.00095 X_1 X_2 + 0.000090 X_1 X_3 + 0.000144 X_2 X_3 \quad (2)$$

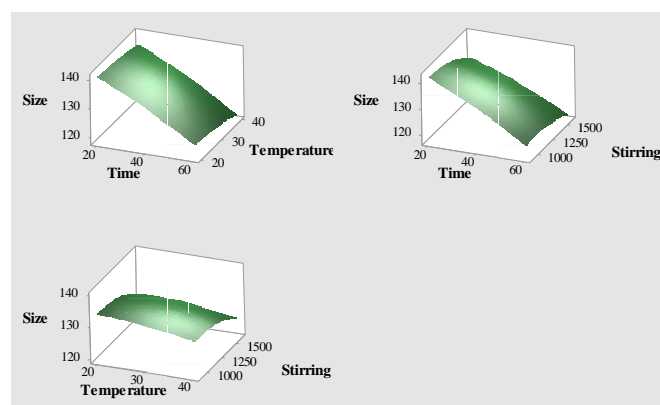
The model summary indicated a coefficient of determination (R²) of 99.23% meaning that the model accounts for 99.23% of the variation in the dependent variable. After adjusting for the number of predictors, the model still explains 97.85% (adjusted R²) of the variation. Furthermore, the model is expected to explain 97.17% (predicted R²) of the variation in the predicted data.

Table 6: The experimental matrix and its corresponding responses

Run	Variable levels		Observed values		
	Temperature (°C)	Time (min)	Velocity (rpm)	Size (nm)	
	(X ₁)	(X ₂)	(X ₃)	(Y)	
1	30	40	1250	130.281	
2	30	40	1250	131.477	
3	30	40	1250	133.580	
4	30	60	900	121.352	
5	40	40	1600	124.604	
6	20	40	900	134.200	
7	40	40	900	130.483	
8	30	20	900	141.846	
9	30	60	1600	117.873	
20	20	40	1600	127.056	
11	20	20	1250	140.870	
12	30	20	1600	134.342	
13	40	20	1250	137.669	
14	40	60	1250	118.685	
15	20	60	1250	122.644	

**Figure 4:** Pareto chart of standardized effects for average droplet size ($\alpha = 0.05$)

The ANOVA results from the RSM analysis average droplet size revealed that the individual factors, mixing temperature, mixing time, and stirring velocity, had statistically significant impacts. Additionally, the quadratic effect of stirring velocity was notably significant (p -value < 0.05), suggesting non-linear interactions. This was further illustrated by the Pareto chart of the standardized effects (Figure 4), highlighting each factors' contribution to droplet size variability. The regression model is validated as suitable, as indicated by the lack-of-fit being insignificant (p -value > 0.05) and the strong alignment between the adjusted and predicted coefficients of determination. Using this model, three-dimensional (3D) surface response plots (Figure 5) were generated to show the relationship between average droplet size and the

**Figure 5:** 3D surface plots for average droplet size in terms of mixing temperature, mixing time, and stirring velocity with the hold values of 30°C, 40 minutes, and 1250 rpm

factors of mixing temperature, mixing time, and stirring velocity. The plots revealed an inverse relationship between these variables and droplet size, with mixing time exerting the most significant effect, followed by stirring velocity and mixing temperature. Formulations 9, 14, 4, and 15 (Table 6) achieved the smallest average droplet sizes, all prepared with a mixing time set at the (+1) level. The response optimizer tool predicted optimal conditions for minimizing particle size, identifying a mixing temperature of 40°C, mixing time of 60 minutes, and stirring velocity of 1600 rpm (Table 7). This resulted in predicting an average droplet size of 115.258 nm. Validation experiments performed in triplicate confirmed the model's accuracy, yielding an average droplet size of 118.973 ± 0.221 nm, aligning closely with the prediction.

Table 7: Solution for response optimization for average droplet size

Solution	Temperature (°C)	Time (min)	Velocity (rpm)	Size Fit (nm)	Composite Desirability
1	40	60	1600	115.258	1

Conclusion

This study represents a novel approach to efficiently formulate Argan oil nanoemulsions using a low-energy method with a single surfactant, aimed at potential dermatological applications. The Argan oil's composition and properties were assessed in accordance with international standards. Stability was evaluated through a pseudo-ternary phase diagram and the phase inversion emulsification method, while optimal process parameters were identified via RSM analysis. The analysis of physicochemical properties and bioactive compounds of Argan oil led to the successful development and characterization of stable nanoemulsions with small droplet sizes. The findings demonstrate that the PIC emulsification technique efficiently produces stable Argan oil nanoemulsions using only one non-ionic surfactant, without requiring additional compounds or high shear speeds. These nanoemulsions show significant potential for dermatological applications. Future studies are recommended to further investigate the bioactivity of these nanoemulsions and evaluate their potential pharmaceutical applications.

Conflict of Interest

The authors declare no conflict of interest.

Authors' Declaration

The authors hereby declare that the work presented in this article is original and that any liability for claims relating to the content of this article will be borne by them.

Acknowledgement

The authors acknowledge the financial support provided by the Research Excellence Scholarships program (Grant 23UAE2020) from the Moroccan National Centre for Scientific and Technical Research (CNRST).

References

- Goik U, Goik T, Zaęska I. The Properties and Application of Argan Oil in Cosmetology. *Eur. J. Lipid Sci. & Technol.* 2019;121(4):1800313; doi: 10.1002/ejlt.201800313.
- Ben Mansour R, Ben Slema H, Falleh H, Tounsi M, Seif Allah Kechebar M, Ksouri R, Megdiche-Ksouri W. Phytochemical characteristics, antioxidant, and health properties of roasted and unroasted Algerian argan (*Argania spinosa*) oil. *J. Food Biochem.* 2018;42(5):e12562; doi: 10.1111/jfbc.12562.
- El Idrissi Y, Moudden HE, El-Guezzane C, Bouayoun T, Dahrouch A, Chahboun N, Zarrouk A, Tabyaoui M. The influence of the forms on the quality, chemical composition and antioxidant activity of argan oil grown in morocco. *J. Microbiol. Biotech. Food Sci.* 2023;e5794; doi: 10.55251/jmbfs.5794.
- Avsar U, Halici Z, Akpinar E, Yayla M, Avsar U, Harun U, Hasan Tarik A, Bayraktutan Z. The Effects of Argan Oil in Second-degree Burn Wound Healing in Rats. *Ostomy Wound Manage.* 2016;62(3):26–34.
- Ben Menni H, Belarbi M, Ben Menni D, Bendiab H, Kherraf Y, Ksouri R, Djebli N, Visioli F. Anti-inflammatory activity of argan oil and its minor components. *Int. J. Food Sci. Nutr.* 2020;71(3):307–314; doi: 10.1080/09637486.2019.1650005.
- Boucetta KQ, Charrouf Z, Aguenau H, Derouiche A, Bensouda Y. The effect of dietary and/or cosmetic argan oil on postmenopausal skin elasticity. *CIA* 2015;339–349; doi: 10.2147/CIA.S71684.
- Demisli S, Theochari I, Christodoulou P, Zervou M, Xenakis A, Papadimitriou V. Structure, activity and dynamics of extra virgin olive oil-in-water nanoemulsions loaded with vitamin D3 and calcium citrate. *J. Mol. Liq.* 2020;306:112908; doi: 10.1016/j.molliq.2020.112908.
- Lococo D, Mora-Huertas CE, Fessi H, Zaanoun I, Elaissari A. Argan Oil Nanoemulsions as New Hydrophobic Drug-Loaded Delivery System for Transdermal Application. *J. of Biomed. Nanotechnol.* 2012;8(5):843–848; doi: 10.1166/jbn.2012.1445.
- Raviadaran R, Chandran D, Shin LH, Manickam S. Optimization of palm oil in water nano-emulsion with curcumin using microfluidizer and response surface methodology. *LWT* 2018;96:58–65; doi: 10.1016/j.lwt.2018.05.022.
- Yang Q, Liu S, Gu Y, Tang X, Wang T, Wu J, Liu J. Development of sulconazole-loaded nanoemulsions for enhancement of transdermal permeation and antifungal activity. *Int. J. Nanomedicine* 2019;14:3955–3966; doi: 10.2147/IJN.S206657.
- Pradiptatiwi GA, Chiuman L, Fadillah Q, Chairunnisa U. Phytochemical, Antibacterial, and Cytotoxic Properties of Suji Plant (*Dracaena angustifolia* [Medik.] Roxb.) Nanoemulsion Serum as Potential Anti-Acne. *Trop. J. Nat. Prod. Res.* 2024;8(7):7688–7692; doi: 10.26538/tjnp/v8i7.9.
- Rai VK, Mishra N, Yadav KS, Yadav NP. Nanoemulsion as pharmaceutical carrier for dermal and transdermal drug delivery: Formulation development, stability issues, basic considerations and applications. *J. Control. Release* 2018;270:203–225; doi: 10.1016/j.jconrel.2017.11.049.
- Prakash V, Parida L. Characterization and rheological behavior of vitamin E nanoemulsions prepared by phase inversion composition technique. *Results Eng.* 2023;18:101175; doi: 10.1016/j.rineng.2023.101175.
- Chaturvedi S, Garg A. Development and optimization of nanoemulsion containing exemestane using box-behnken design. *J. Drug Deliv. Sci. Technol.* 2023;80:104151; doi: 10.1016/j.jddst.2023.104151.
- Cunha FVM, de Medeiros ASA, dos Santos Silva AM, de Morais MC, de Sousa PD, de Assis Oliveira F, da Silva Júnior AA, Nunes LCC. Ethylferulate-loaded nanoemulsions as a novel anti-inflammatory approach for topical application. *J. Mol. Liq.* 2023;369:120733; doi: 10.1016/j.molliq.2022.120733.
- Wang X, Fu L, Cheng W, Chen J, Zhang H, Zhu H, Zhang C, Fu C, Hu C, Zhang J. Oral administration of Huanglian-Houpo herbal nanoemulsion loading multiple phytochemicals for ulcerative colitis therapy in mice. *Drug Deliv.* 2023;30(1):2204207; doi: 10.1080/10717544.2023.2204207.
- Asmawi AA, Salim N, Abdulmalek E, Abdul Rahman MB. Size-Controlled Preparation of Docetaxel- and Curcumin-Loaded Nanoemulsions for Potential Pulmonary Delivery. *Pharmaceutics* 2023;15(2):652; doi: 10.3390/pharmaceutics15020652.
- Sindi AM, Hosny KM, Rizg WY, Sabei FY, Madkhali OA, Bakkari MA, Alfayez E, Alkharobi A, Alghamdi SA, Banjar AA, Majrashi M, Alissa M. Utilization of experimental design in the formulation and optimization of hyaluronic acid-based nanoemulgel loaded with a turmeric–curry leaf oil nanoemulsion for gingivitis. *Drug Deliv.* 2023;30(1):2184311; doi: 10.1080/10717544.2023.2184311.
- International Standardization Organization. Animal and vegetable fats and oils - Determination of acid value and acidity. ISO Standard No 660:2020 2020.
- International Olive Council. Determination of Peroxide value. Method COI/T20/Doc No 35 2017.
- International Standardization Organization. Animal and vegetable fats and oils - Determination of ultraviolet absorbance expressed as specific UV extinction. ISO Standard No 3656:2011 2011.
- International Standardization Organization. Animal and vegetable fats and oils - Determination of iodine value. ISO Standard No 3961:2018 2018.
- International Standardization Organization. Animal and vegetable fats and oils - Determination of saponification value. ISO Standard No 3657:2020 2020.
- International Standardization Organization. Animal and vegetable fats and oils - Determination of unsaponifiable matter. ISO Standard No 3596:2000 2000.
- International Standardization Organization. Animal and vegetable fats and oils - Determination of conventional mass per volume (litre weight in air). ISO Standard No 6883:2017 2017.

26. International Standardization Organization. Animal and vegetable fats and oils - Determination of refractive index. ISO Standard No 6320:2017 2017.
27. International Standardization Organization. Animal and vegetable fats and oils - Determination of moisture and volatile matter content. ISO Standard No 662:2016 2016.
28. International Standardization Organization. Animal and vegetable fats and oils - Determination of insoluble impurities content. ISO Standard No 663:2017 2017.
29. International Standardization Organization. Animal and vegetable fats and oils - Determination of anisidine value. ISO Standard No 6885:2016 2016.
30. International Olive Council. Determination of fatty acid methyl esters by gas chromatography. Method COI/T20/Doc No 33 2017.
31. International Standardization Organization. Animal and vegetable fats and oils - Determination of tocopherol and tocotrienol contents by high-performance liquid chromatography. ISO Standard No 9936:2016 2016.
32. Kamal R, Kharbach M, Vander Heyden Y, Doukkali Z, Ghchime R, Bouklouze A, Cherrah Y, Alaoui K. *In vivo* anti-inflammatory response and bioactive compounds' profile of polyphenolic extracts from edible Argan oil (*Argania spinosa L.*), obtained by two extraction methods. *J. Food Biochem.* 2019;43(12): e13066; doi: 10.1111/jfbc.13066.
33. Borello E, Domenici V. Determination of Pigments in Virgin and Extra-Virgin Olive Oils: A Comparison between Two Near UV-Vis Spectroscopic Techniques. *Foods* 2019;8(1):18; doi: 10.3390/foods8010018.
34. Gul U, Khan MI, Madni A, Sohail MF, Rehman M, Rasul A, Peltonen L. Olive oil and clove oil-based nanoemulsion for topical delivery of terbinafine hydrochloride: *in vitro* and *ex vivo* evaluation. *Drug Deliv.* 2022;29(1):600–612; doi: 10.1080/10717544.2022.2039805.
35. Li X, Wu G, Qi X, Zhang H, Wang L, Qian H. Physicochemical properties of stable multilayer nanoemulsion prepared via the spontaneously-ordered adsorption of short and long chains. *Food Chem.* 2019;274:620–628; doi: 10.1016/j.foodchem.2018.09.002.
36. Ahmad N, Ansari K, Alamoudi MK, Ullah Z, Haque A, Ibrahim HO. Development of novel nanoemulsion of pioglitazone used in the treatment of diabetes and its gel form for the treatment of skin diseases. *J. Drug Deliv. Sci. Technol.* 2024;100:106096; doi: 10.1016/j.jddst.2024.106096.
37. Moroccan Standards Institute. Animal and vegetable fats and oils – Argan oil – Specifications. NM 085090 2003.
38. Čizinauskas V, Elie N, Brunelle A, Briedis V. Fatty acids penetration into human skin *ex vivo*: A TOF-SIMS analysis approach. *Biointerphases* 2017;12(1):011003; doi: 10.1116/1.4977941.
39. Şekeroğlu ZA, Aydın B, Şekeroğlu V. Argan oil reduces oxidative stress, genetic damage and emperipolesis in rats treated with acrylamide. *Biomed. & Pharmacother.* 2017;94:873–879; doi: 10.1016/j.biopha.2017.08.034.
40. Hanana M, Mezghenni H, Ben Ayed R, Ben Dhiab A, Jarradi S, Jamoussi B, Hamrouni L. Nutraceutical potentialities of Tunisian Argan oil based on its physicochemical properties and fatty acid content as assessed through Bayesian network analyses. *Lipids Health Dis.* 2018;17(1):138–148; doi: 10.1186/s12944-018-0782-9.
41. Yusuf VAJ, Soeratri W, Erawati T. The Effect of Surfactant Combination on the Characteristics, Stability, Irritability, and Effectivity of Astaxanthin Nanoemulsion as Anti-Ageing Cosmetics. *Trop. J. Nat. Prod. Res.* 2023;7(12):5509–5518; doi: 10.26538/tjnpr/v7i12.21.
42. Kamaruzaman N, Yusop SM. Determination of stability of cosmetic formulations incorporated with water-soluble elastin isolated from poultry. *J. King Saud Univ. Sci.* 2021;33(6):101519; doi: 10.1016/j.jksus.2021.101519.
43. Duarte J, Sharma A, Sharifi E, Damiri F, Berrada M, Khan MA, Singh SK, Dua K, Veiga F, Mascarenhas-Melo F, Pires PC, Paiva-Santos AC. Topical delivery of nanoemulsions for skin cancer treatment. *Appl. Mater. Today* 2023;35:102001; doi: 10.1016/j.apmt.2023.102001.